Journal of Magnetism and Magnetic Materials 322 (2010) 2227–2230

Contents lists available at ScienceDirect

Journal of Magnetism and Magnetic Materials

journal homepage: www.elsevier.com/locate/jmmm

Magnetism in nanoparticles of semiconducting $FeSi_2$

H.H. Hamdeh [a], M.M. Eltabey [a,1], J.C. Ho [a], P.C. Lee [b,c], K. Chen [b], Y.Y. Chen [b,d,*]

[a] Department of Physics, Wichita State University, Wichita, KS, USA
[b] Institute of Physics, Academia Sinica, Taipei 11529, Taiwan, ROC
[c] Department of Engineering and System Science, National TsingHua University, Hsinchu 30013, Taiwan, ROC
[d] Graduate Institute of Applied Physics, National Chengchi University, Taipei 11605, Taiwan, ROC

ARTICLE INFO

Article history:
Received 21 May 2009
Received in revised form
1 February 2010
Available online 13 February 2010

Keywords:
Iron disilicide
Nanoparticle
Mössbauer
Specific heat

ABSTRACT

Iron disilicide has been found to exhibit superparamagnetism in nanoparticles, even though no magnetic ordering occurs in bulk. The unexpected behavior was attributed, based on magnetic studies, to chemical disorder. A lack of sextet-type signals in Mössbauer spectra supports that the observed magnetic order is confined to only a very small fraction of magnetic Fe ions. Moreover, quadrupole-splitting and isomer-shift parameters reveal a significant amount of Fe in a short-range α-$FeSi_2$ structure, while XRD suggests an overall β-$FeSi_2$ structure. Such a compositional heterogeneity is also reflected in a calorimetrically obtained spin-glass-like anomaly at low temperatures. Meanwhile, as the particle size decreases, specific heat and Sommerfeld constant are enhanced due to lattice softening and the emergence of surface charge density of states, respectively, in nanoparticles.

1. Introduction

Iron in bulk Fe_xSi_{1-x} carries a sizable magnetic moment and undergoes a ferromagnetic transition above 500 °C only if $x \geq 0.5$ [1]. With a much lower Fe content with x=0.33, iron disilicide exhibits no magnetic ordering. The ambient-temperature stable β-$FeSi_2$ is a narrow-gap semiconductor and has been well recognized for potential applications from thermoelectric devices and solar cells [2] to optoelectronics [3]. After being formed into nanoscale particles, it was found to behave superparamagnetically with blocking temperatures ranging from 8 to 34 K for 15–55 nm, respectively [4]. The unexpected behavior was attributed to chemical disorder induced during fabrication of nanoparticles. Specifically, the observed magnetism could be associated with a small fraction of Fe ions, which have a sufficient number of other Fe as close neighbors, thus satisfying the $x \geq 0.5$ condition to exhibit magnetism. If such a compositional-heterogeneity magnetism is indeed a common feature of multi-element materials, it could very well enhance the viable advantages of magnetic application in semiconductor nanotechnology. The recent discovery of ferrimagnetism in nanoparticles of zinc ferrite, which is antiferromagnetic in bulk, is a good example [5].

For $FeSi_2$ the supporting evidence of chemical disorder came mainly from the relatively low saturation magnetization [4]. It is necessary using different approaches to verify the conclusion. In this work, Mössbauer spectroscopic and low-temperature calorimetric measurements were employed to attain the confirmation.

2. Experimental

Nanoparticles of size d=22, 40, and 55 nm were fabricated by ArF excimer laser ablation of the bulk β-$FeSi_2$ as target. The details of sample fabrication are the same as those in the previous report [4], which gives a complete description of the material synthesis and characterization including X-ray diffraction, transmission electron microscopy, and a series of magnetic measurements. From XRD patterns the structure of nanoparticles remains the same as that of bulk compound, consistent with EDS data showing close to 1:2 ratio between Fe and Si.

^{57}Fe Mössbauer effect measurements on a 22 nm sample were carried out at 300 and 4.2 K, respectively, with a conventional constant acceleration spectrometer. Absorbers were prepared by dispersing samples evenly between two pieces of thin plastic tapes. A gamma-ray source of 50-mCi ^{57}Co in a rhodium matrix was used and transmission spectra were obtained with a gas detector.

Thermal relaxation-type calorimetric measurements [6,7] were made between 0.3 and 35 K in a ^{3}He cryostat. In each experiment, a milligram sample was thermal anchored with a minute amount of N-grease to a tiny sapphire disk. Thin films of RuO_2/Al_2O_3 and Ni–Cr were deposited on the sapphire to serve as thermometer and heater, respectively. The relatively small heat

* Corresponding author. Tel.: +886 2 2789 6725; fax: +886 2 2783 4187.
E-mail address: cheny2@phys.sinica.edu.tw (Y.Y. Chen).
[1] On leave from Basic Engineering Science Department, Menoufia University, Shbein, Egypt.

0304-8853/$ - see front matter © 2010 Elsevier B.V. All rights reserved.
doi:10.1016/j.jmmm.2010.02.015

capacity of this sample holder $C_{addenda}$ was separately measured for addenda corrections. The sapphire disk was suspended by four Au–Cu wires to a copper block as thermal links. For each measurement, the temperature of copper block was first stabilized. A small amount of Joule heat was introduced to the sample holder, followed by a fast thermal relaxation to the copper block. The sample temperature was fitted to exponential time dependence to yield a time-constant τ. The heat capacity was calculated from the expression $C=\kappa\tau$, where κ is the thermal conductance of Au–Cu wires. Uncertainties in precision and accuracy were estimated to be about 3%.

3. Results and discussion

Mössbauer effect measurements provide valuable information the structure, electronic valence, and magnetic states of atoms in solids. Each Mössbauer spectrum as obtained from the resonant and recoil-free emission, and absorption of gamma rays by nuclei can have three basic components. Isomer-shift (IS) of the nuclear energy levels arises from the Coulomb potential between the nucleus and the surrounding electron cloud, which depends strongly on the electronic valence state. Quadruple-splitting (QS), yielding a doublet in the spectrum, reflects the asymmetry in electric field gradient of the electron cloud and is, therefore, structure sensitive. A magnetic-hyperfine-field (MHF), which is caused primarily by the exchange interaction of s-like electrons at the nucleus and the unpaired 3d-electrons local to the Fe-atom, prevails only if the magnetic moments of the 3d-electrons are fixed in space during the measurement time of approximately 10^{-9} s. MHF would yield a sextet spectrum. Most relevant to local variation studies is the short-range-order (SRO) nature of quadrupole splitting, in contrast to other evaluation techniques such as XRD reflecting structure of long-range-order.

The experimental data in Fig. 1 have no identifiable sextet beyond the background noise. This agrees with the previous conclusion, based on saturation magnetization data, of large chemical disorder in the material. Indeed, if only few percentages of Fe atoms retain large magnetic moments, then the signal from these atoms will be shallow and difficult to observe. On the other hand, the features of the two doublets exhibited in both 300 and 4.2 K spectra indicate wide distributions of the quadruple-splitting and isomer-shift. To obtain these parameters, the experimental data were fitted by two independent methods. In the first method proposed by Le Caer and Dubois [8], a linear relation between IS (relative to pure Fe) and QS is assumed. A relation IS = −0.787 + 1.686 QS was determined from the best fit of the calculated spectrum to the experimental one. In the second method, the experimental data were fitted to the sum of two doublets of Lorentz lines having the same broad width. The IS and QS of each were freely adjusted in the fitting routine. The average values of IS and QS obtained by the second method are in good agreement with the peak values obtained by the first method. These values are summarized in Table 1.

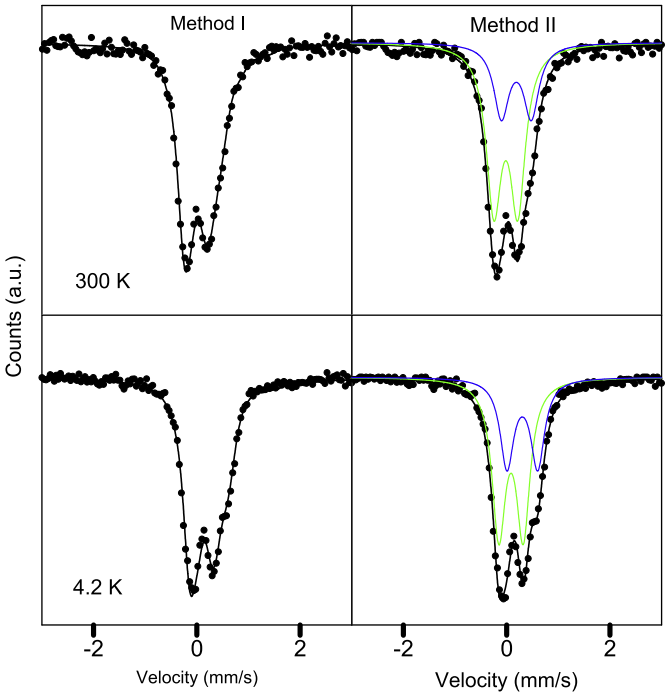

Fig. 1. Mössbauer spectra of 22-nm $FeSi_2$ at 300 or 4.2 K, each fitted with the method of (i) Le Caer and Dubois (the left) or (ii) two doublets (i.e., two fitting subspectra as shown, representing two non-equivalent Fe sites) of Lorentz lines (the right).

The calculated QS distributions shown in Fig. 2 extend from 0.35 to 0.70 mm/s, and thus correspond to a distribution of low symmetry Fe sites. Distinct peaks, however, point to two different short-range-order environments. In $FeSi_2$, there are two known stable structures, namely the orthorhombic β-$FeSi_2$ and the tetragonal α-$FeSi_2$. Both structures have sublattices of deformed Si cubes. The β-structure contains two non-equivalent Fe sites of equal occupation, whereas the α-structure is developed from the β-structure by the formation of Fe vacancies [9]. Previous work [10,11] showed that the distortions of the Si cubes are sensitive to the preparation methods as indicated by the different QS values reported from β-$FeSi_2$ grown by molecular beam epitaxy and from powdered solid state reaction material. The QS values for the two different Fe sites were reported at −0.315 and 0.525 mm/s in the epitaxial grown film [10], and at 0.41 and 0.43 mm/s in the powdered material [11]. On the other hand, the QS values in α-$FeSi_2$ ranged from 0.4 to 0.7 mm/s [11]. This distribution was attributed to the number of Fe vacancies in the nearest, or next nearest, neighbor shell of a central Fe atom. Using this information along with the XRD pattern that reveals the β-phase, we can reasonably associate the major peak of the QS distribution with the β-phase, and the minor peak with the α-phase. This short-range-order (SRO) identification of quadrupole splitting is also supported by the match of IS values reported here for both phases and those in previous studies [10,11].

The populations of the Fe sites describing the SRO could be determined from the areas of the peaks in the QS distribution. To obtain these parameters, the QS distribution, at 4.2 K, was best fitted to two independent skewed Gaussian functions. The calculated areas from both methods are listed in Table 1. Note that the computed areas at 4.2 K reflects best of the SRO parameters because at 4.2 K, there is less overlapping between

Table 1
Analysis of quadrupole-splitting and isomer-shift parameters based on two different methods. Also obtained are relative percentages of two components at 4.2 K.

	Temperature (K)	QS (mm/s)	IS (mm/s)	Area (%)
Method I	300	0.45	0.08	–
		0.59	0.32	–
	4.2	0.46	–	68
		0.60	–	32
Method II	300	0.46	0.09	–
		0.57	0.29	–
	4.2	0.47	–	64
		0.59	–	36

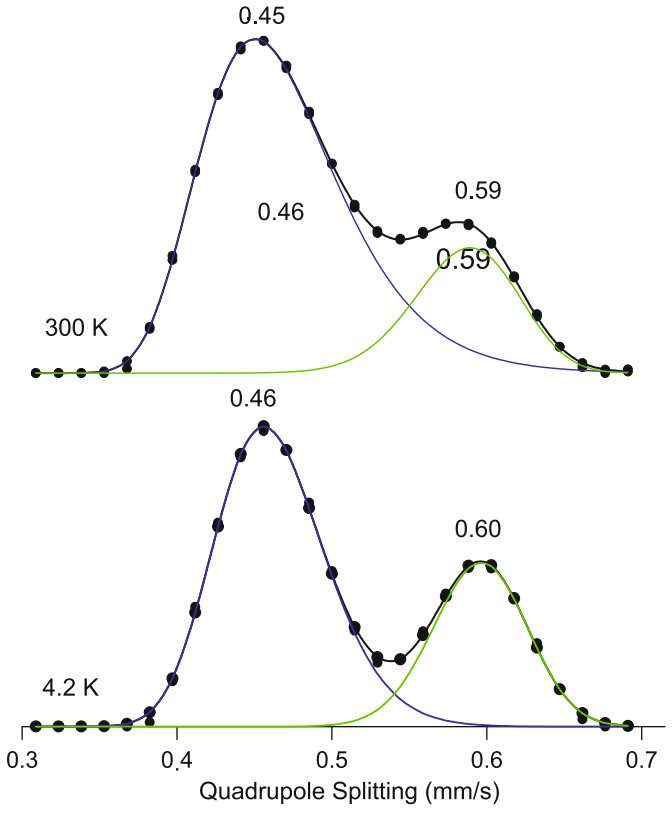

Fig. 2. Quadrupole-splitting distribution from 4.2-K Mössbauer data, yielding two components with short-range-order corresponding to α-$FeSi_2$ (green peak) and β-$FeSi_2$ (blue peak). (For interpretation of the references to colour in this figure legend, the reader is referred to the web version of this article.)

the two peaks and the recoil free fraction is the same for all Fe sites.

The QS of the peaks representing the SRO remain independent of temperature but the width and the shape have changed significantly. This behavior leads to two significant conclusions. First, QS is caused primarily by the lattice, and the observed changes may be due to thermally induced lattice distortions. Second, these distortions are not simply thermal contractions but distortions crystallizing the two SROs. They appear to be a Jahn–Teller type distortion towards equilibrium. As mentioned above, however, magnetic perturbations may have taken place too. Both α- and β-bulk phases are reported to be paramagnetic. Considering the relation between the IS and the Fe valance electrons, and thus the Fe magnetic moment, the IS values may point to a larger magnetic moment of Fe in the α-phase than in the β-phase. The increase in IS results from a decrease in the contact charge density, and it could be caused by direct reduction in the density of s-like electrons or indirectly by the increase in 3d-electrons.

The specific heat data below 35 K for bulk and 22, 40 and 55 nm samples are shown in Fig. 3. Normally the specific heat of a solid has a lattice (C_l) and an electronic (C_e) contribution, which are roughly equal to βT^3 and γT, respectively, at low temperatures.

1However, an additional contribution prevails at lower temperatures. It is believed to be a magnetic contribution and will be discussed below. The total specific heat can be formulated as

$$C = C_l + C_e + C_m \quad (1)$$

where C_m is the magnetic contribution of spin-glass-like anomaly. Using a more precise analysis similar to the description in a previous report [12], the Debye function for C_l was applied. The temperature dependence of Debye temperature θ_D and

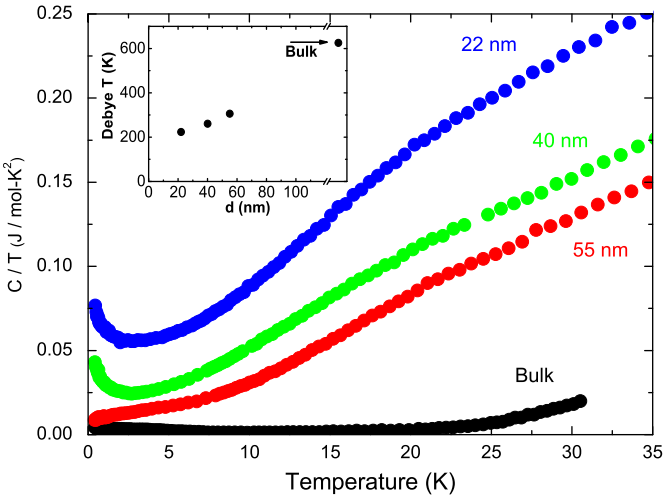

Fig. 3. Temperature dependence of C/T, showing an anomalous contribution to specific heat below about 10 K, which becomes more pronounced as nanoparticle size decreases. Inset: Size dependence of Debye temperature.

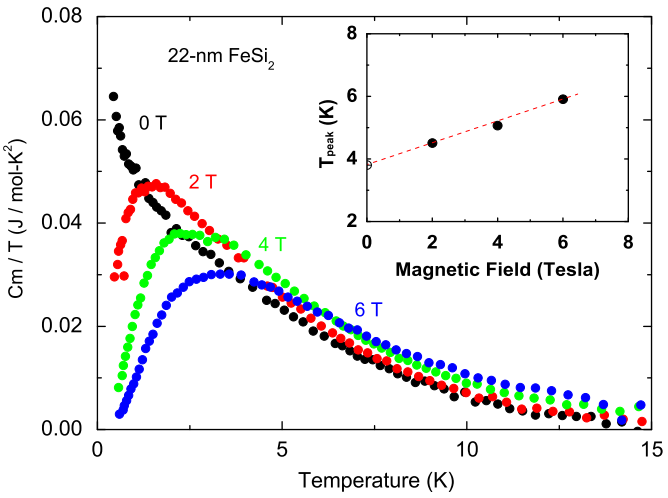

Fig. 4. Temperature dependence of C_m/T of spin-glass-like anomaly in 22-nm sample for various fields. Inset: Peak-position shifted linearly to higher temperature with magnetic field.

Sommerfeld constant γ were derived. The fact that θ_D decreases with size reduction as shown in the insets of Fig. 3 arises as size-dependent lattice softening, which has been observed in, e.g., $ZnFe_2O_4$ [13] and $CeAl_2$ [14]. By subtracting the lattice phonon and electronic contributions, the magnetic component of the spin-glass-like anomaly can be extracted. The result of the 22 nm sample is shown in Fig. 4. Meanwhile, the $1/d$ dependence of Sommerfeld constant in the inset of Fig. 5 may be an indication of the charge density of states created in the surface of nanoparticles with expected structural disorders or defects.

The spin-glass-like transition is evidenced by the specific heat measurements in magnetic field. Fig. 4 shows the anomaly for the 22 nm sample shifts to higher temperatures with an applied magnetic field of 2 T or above. This is the characteristic behavior of a spin-glass-like transition under magnetic field [15], which can easily be anticipated to occur in nanoparticles here containing only a small magnetic fraction of Fe_xSi_{1-x} with $x > 0.5$. The temperature T_{peak} defined by the peak position of the specific heat anomaly is also shown in the inset of Fig. 4. The linearly shifted T_{peak} to higher temperature with magnetic field is similar to the results in the other literature [16]. To estimate the magnetic

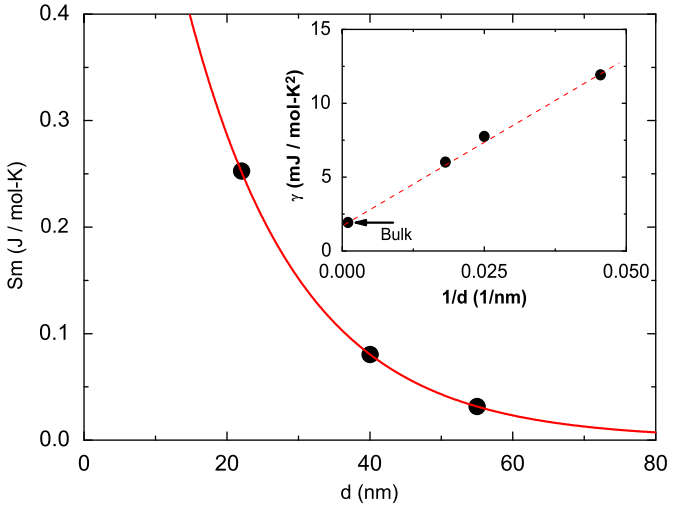

Fig. 5. Size dependence of magnetic entropy for nanoparticles. Inset: The Sommerfeld constant is linear proportional to $1/d$.

fraction of the spin-glass-like transition, the entropy change associated with the magnetic anomaly was estimated based on the formula

$$S_m = \int (C_m/T)dT \quad (2)$$

Unlike magnetization, which is vulnerable to magnetic frustration and canting, the entropy derived from specific heat as a statistical thermodynamic quantity reflects actual degree of disorder. In general, for a completely disordered state $S_m = R \ln \Omega$ per mole, with Ω being the spin-state multiplicity such as 2 and $S_m = 5.8$ J/mol K for the ground state $J = 1/2$ for Fe^{3+} ion. The drastically increased magnetic entropy with size reduction (Fig. 5) in turn reflects the size effect on chemical disorders. The rather low S_m values (< 0.3 J/mol K) confirm that only a very small fraction of Fe_xSi_{1-x} ($x > 0.5$) in the nominally $FeSi_2$ sample exhibits the superparamagnetic behavior. For the 22 nm sample with $S_m = 0.25$ J/mol K, the fraction is estimated to be about 4.3%. Again, this is consistent with the Mössbauer spectroscopic data mentioned above.

In conclusion, the observed chemical-disorder induced magnetism in nanoparticles of $FeSi_2$ is indeed confined to a small magnetic fraction of $Fe_xSi_{1-x}(x > 0.5)$ by Mössbauer spectroscopic analysis and measurements of specific heat. Based on entropy calculation of spin-glass-like anomaly, its fraction is estimated to be about 4.3% for the 22 nm sample.

Acknowledgment

Work at Academia Sinica was supported by the National Research Council, the Republic of China, under Grant No. NSC 97-2120-M-001-007.

References

[1] O. Kubaschewski, in: Iron-Binary Phase Diagrams, Springer, New York, 1982 p. 136.
[2] E. Muller, C. Drasar, J. Schliz, W.A. Kaysser, Mater. Sci. Eng. A 362 (2003) 17.
[3] D. Leong, M. Harry, J. Reeson, K.P. Homewood, Nature (London) 387 (1997) 686.
[4] Y.Y. Chen, P.C. Lee, C.B. Tsai, S. Neeleshwar, C.R. Wang, J.C. Ho, H.H. Hamdeh, Appl. Phys. Lett. 91 (2007) 251907.
[5] H.H. Hamdeh, J.C. Ho, S.A. Oliver, J. Appl. Phys. 81 (1851) 1997.
[6] Y.Y. Chen, Temperature: Its Measurement and Control in Science and Industry, vol. 7, American Institute of Physics, New York, 2003, p. 387.
[7] Y.Y. Chen, P.C. Chen, C.B. Tsai, K.I. Suga, K. Kindo, Int. J. Thermophys. 30 (2009) 316–324.
[8] G. Le Caër, J.M. Dubois, J. Phys. E 12 (1979) 1083.
[9] Y. Dusausoy, J. Protas, R. Wandji, B. Roques, Acta Crystallogr. B27 (1971) 1209.
[10] M. Fanciulli, C. Rosenblad, G. Weyer, A. Svane, N.E. Chritensen, Phys. Rev. Lett. 75 (1642) 1995.
[11] C. Blaauw, F. van der Woude, G.A. Sawatzky, J. Phys. C 6 (1973) 2371.
[12] Y.Y. Chen, P.H. Huang, Y.D. Yao, T.K. Lee, M.N. Ou, M.Y. Ho, J.M. Lawrence, C.H. Booth, Phys. Rev. Lett. 98 (2007) 157206.
[13] J.C. Ho, H.H. Hamdeh, Y.Y. Chen, S.H. Lin, Y.D. Yao, R.J. Willey, S.A.O. Oliver, Phys. Rev. B 52 (1995) 10122.
[14] Y.Y. Chen, Y.D. Yao, C.R. Wang, W.H. Li, C.L. Chang, T.K. Lee, T.M. Hong, J.C. Ho, S.F. Pan, Phys. Rev. Lett. 84 (2000) 4990.
[15] E.V. Sampathkumaran, N. Mohapatra, S. Rayaprol, K.K. Iyer, Phys. Rev. B 75 (2007) 052412.
[16] A.P. Ramirez, B. Hessen, M. Winklemann, Phys. Rev. Lett 84 (2000) 2957.